Published in final edited form as:

Curr Osteoporos Rep. 2016 August ; 14(4): 138–150. doi:10.1007/s11914-016-0314-3.

Tissue-level Mechanical Properties of Bone Contributing to Fracture Risk

Jeffry S. Nyman[1,2,3,4], **Mathilde Granke**[1,3], **Robert C. Singleton**[5], and **George M. Pharr**[5,6]

[1]Department of Orthopaedic Surgery & Rehabilitation, Vanderbilt University Medical Center, Nashville, TN 37232

[2]Department of Veterans Affairs, Tennessee Valley Healthcare System, Nashville, TN 37212

[3]Center for Bone Biology, Vanderbilt University Medical Center, Nashville, TN 37232

[4]Department of Biomedical Engineering, Vanderbilt University, Nashville, TN 37232

[5]Materials Science and Engineering Department, University of Tennessee, Knoxville, TN 37996

[6]Materials Science and Technology Division, Oak Ridge National Laboratory, Oak Ridge, TN 37831

Abstract

Tissue-level mechanical properties characterize mechanical behavior independently of microscopic porosity. Specifically, quasi-static nanoindentation provides measurements of modulus (stiffness) and hardness (resistance to yielding) of tissue at the length scale of the lamella, while dynamic nanoindentation assesses time-dependent behavior in the form of storage modulus (stiffness), loss modulus (dampening), and loss factor (ratio of the two). While these properties are useful in establishing how a gene, signaling pathway, or disease of interest affects bone tissue, they generally do not vary with aging after skeletal maturation or with osteoporosis. Heterogeneity in tissue-level mechanical properties or in compositional properties may contribute to fracture risk, but a consensus on whether the contribution is negative or positive has not emerged. In vivo indentation of bone tissue is now possible, and the mechanical resistance to microindentation has the potential for improving fracture risk assessment, though determinants are currently unknown.

Keywords

nanoindentation; hardness; viscoelasticity; bound water; bone quality; spectroscopy

Corresponding Author: Jeffry S. Nyman, 1215 21st Ave. S., South Tower, Suite 4200, Nashville, TN 37232, jeffry.s.nyman@vanderbilt.edu, office: (615) 936-6296, fax: (615) 936-0117.

Compliance with Ethics Guidelines

Conflict of Interest

Jeffry S. Nyman reports grants from NSF, grants from NIH, and grants from VA, during the conduct of the study; In addition, Dr. Nyman is co-inventor on US Patent 8,923,948 System and method for determining mechanical properties of bone structures issued. Mathilde Granke and Robert C. Singleton declare that they have no conflict of interest. George M. Pharr reports grants from NSF, during the conduct of the study.

Human and Animal Rights and Informed Consent

This article does not contain any studies with human or animal subjects performed by any of the authors.

Introduction

In the hierarchical organization of bone, *tissue-level* mechanical properties are measured in way that is independent of macrostructure and microstructure. Whether acquired from cortical or trabecular tissue, they depend on the ultrastructural organization of type I collagen fibrils infused with semi-crystalline, carbonated hydroxyapatite and not microscopic porosity (e.g, Haversian canals). As such, the putative determinants of the mechanical behavior of bone tissue include: collagen orientation, collagen crosslinking profile, degree of mineralization or mineral-to-matrix ratio, bound water, and mineral structure (Table 1). These same compositional characteristics also influence *apparent-level* mechanical properties that are determined from monotonic or dynamic tests of uniform, machined samples of bone (e.g., beam or parallelepiped, 'dog-bone', cylindrical, etc.) or estimated from flexural tests of whole-bone in which the structure (e.g., moment of inertia or cross-sectional area) is known. However, such apparent-level properties as strength and toughness also depend on the bulk characteristics of porosity and cement lines. Because bone tissue is heterogeneous in its primary constituents (i.e., organic matrix and mineral), the relationships between local tissue-level mechanical properties and overall fracture resistance are not readily quantifiable. Herein, how tissue-level mechanical properties do and do not contribute to fracture risk is discussed.

Tissue-level mechanical properties provide insight into how diseases, genes, and growth factors, affect bone with respect to mechanical function of the extracellular matrix [1, 2]. They do not necessarily indicate whether a bone is weak or strong or whether it is brittle or tough as the changes in the bone matrix (e.g, higher degree of mineralization or greater concentration of non-enzymatic collagen crosslinks) affect failure mechanisms in ways that are not necessarily reflected in common tissue-level mechanical properties. Nonetheless, the *clinical* importance of tissue to fracture resistance is apparent from the literature on predictors of fracture risk as well as genetic diseases affecting bone matrix (e.g., osteogenesis imperfecta) or mineralization (e.g., hypophosphatasia). As determined by high-resolution, peripheral quantitative computed-tomography (HR-pQCT) or micro-magnetic resonance imaging (μMRI), measurements of cortical thickness, cross-sectional area, volumetric bone mineral density (vBMD), porosity, and trabecular bone volume fraction acquired at distal sites significantly differ between individuals with osteoporotic fractures and those without fractures [3–5]. However, there is overlap in all structural and architectural measurements of bone between these two groups such that there is no one bone property – including the gold-standard areal bone mineral density (aBMD) [6] – that unequivocally predicts fracture risk. This also is the case for strength predictions determined from finite element analysis of the proximal femur [7–9], distal radius [4, 10], and spine [11, 12]. Thus, bone structure and density are not the only factors dictating an individual's risk of fracture because age- and disease-related changes in tissue affect toughening mechanisms, irrespective of changes to cortical structure and trabecular architecture. Information on the contribution of the extracellular matrix to fracture resistance can be found in previous reviews [13, 14].

Measurements of tissue-level mechanical properties of bone often involve load and depth sensing indentation techniques (e.g., nanoindentation and instrumented microhardness

testing) because of the difficulty in generating small uniform specimens of bone tissue for mechanical testing. With microhardness testing, conventional instruments have sensors to generate force (P) vs. displacement (h) curves as the indenter loads and unloads the tissue. From these curves, the tissue hardness (H) and elastic modulus (E) can be determined at scales of ~5 μm to ~200 μm, in which the maximum depth of the indent is dictated by the maximum indentation force (typically 0.1 N – 3 N). Thus, H and E of interstitial and osteonal sites can be assessed separately. Typically made out of diamond, microindenter tips have various geometries with the Vickers four-sided pyramid being a common tip used in bone research. With nanoindentation, tissue H and E are determined at smaller length scales, typically ~0.1 μm to ~10 μm, in which the depth of penetration is usually specified (force typically varies from 1 mN to 25 mN [2]), though a maximum force can also be specified. At these lower forces, individual lamellae can be indented. A Berkovich diamond tip (a three-sided pyramid with the same depth to cross-sectional area as the Vickers indenter) is widely used, though cube corner (diamond) and spherical (diamond or steel) tips have also been applied to the nano-mechanical testing of bone tissue.

In the measurement of P vs. h (Fig. 1a), the contact area between the tip and material is a known function of h [1]. This necessitates that the bone surface be ground and polished to minimize surface roughness and that a calibration standard (e.g., fused quartz) be indented to establish the contact area function of the indenter tip (tips are blunted, not ideal geometric shapes). H is simply the force at the maximum penetration depth divided by the contact area (Fig. 1a), whereas E depends on the unloading stiffness (Fig. 1a), contact area, and several geometry and material characteristics of the tip [15]. Typically, upon reaching the specified depth or target force, there is a dwell period (10 s to 60 s) in which the force remains constant prior to unloading to account for the viscoelastic nature of bone tissue. Creep and viscoelastic analyses can be performed during this dwell period provided there is no contribution to the measured displacements from thermal expansion or contraction of the testing system, or “thermal drift” [16]. Also, since nanoindenters are designed to minimize vibration and precisely control force, a small oscillatory load can be super-imposed onto the static load during the first dwell (Fig. 1b), thereby providing other viscoelastic properties (storage modulus or E', loss modulus or E'', and the loss factor or tan $\delta = E''/E'$) from the phase-shift (δ) between oscillating component of the input load and the displacement response (Fig. 1b) [17].

There are currently two instruments – BioDent™ and OsteoProbe® (ActiveLife Scientific, Inc. Santa Barbara, CA) – capable of indenting human bone tissue *in vivo* [18, 19]. Unlike the aforementioned indentation techniques, a smooth bone surface is not required. Although the loading mechanism differs between the two instruments [20, 21], they each assess the ability of bone to resist the penetration of a 90° conical-spherical, stainless steel tip (2.5 μm and 10 μm radius, respectively). With the BioDent, the periosteal bone is cyclically loaded at 2 Hz between 0 N and a target force, typically 10 N, for 10 to 20 cycles with a load profile similar to nanoindentation (load-to-maximum force, dwell, unload-to 0 N, with each part of the cycle having the same duration of 167 ms). A number of tissue resistance properties can be derived from the resulting force vs. displacement curves (see [22] for details). Whereas the BioDent has a stand to hold the indentation module over the patient’s bone, the OsteoProbe is a hand-held device that generates a one-time, impact load (from 10 N, the

triggering force, to ~ 40 N in 0.25 ms) such that the recorded depth of the tip into the bone (150 μm – 260 μm) is indexed to the harmonic mean of multiple indentation depths into a plastic standard (PMMA). Thus, this instrument provides bone material strength index (BMSi = 100 × PMMA indentation depth per bone indentation depth). Despite its name, BMSi is not necessarily a measure of material strength, though conceivably strong bone tissue would have high BMSi. Also, the assessment of indentation resistance is not necessarily independent of porosity as with traditional tissue indentation tests because pores cannot be purposely avoided. For the most part, cortical bone loss with aging or menopause occurs primarily through endocortical resorption [23], but indentation depth at the periosteal surface of cadaveric tibia mid-shafts (left and right combined) was recently correlated with regional cortical porosity as determined by micro-computed tomography with a voxel size of 30 μm ($r=0.290$, $p=0.043$ for indentation distance increase vs. porosity and $r=-0.299$, $p=0.037$ for BMSi vs. porosity) [24].

Other reviews have summarized the extrinsic factors (e.g., sample preparation, hydration, loading conditions) that affect micro- and nano-indentation properties in addition to the various methods of calculating tissue-level mechanical properties [1, 2, 15], and so the present review discusses studies that used indentation techniques to establish associations between tissue-level mechanical properties and fracture resistance. This includes the few studies that used the non-traditional indentation techniques introduced above – cyclic reference point indentation (cRPI, BioDent) and impact microindentation (IMI, OsteoProbe) – as well as nanoscratch which characterizes in situ toughness. To address the possible contribution of heterogeneity to fracture risk, the present review also includes tissue-level composition from imaging/spectroscopy – quantitative back-scattered electron imaging (qBEI) and Fourier transform infrared imaging (FTIR) – as these tools have been applied to clinical bone samples to a greater extent than micro/nanoindentation.

Independence of tissue-level mechanical properties from donor age, not tissue age

From quasi-static, load-to-failure tests (flexural and tension) of uniform samples of cortical bone extracted from cadavers [25–29], we know that apparent-level mechanical properties such as strength, post-yield toughness, and fracture toughness decrease throughout lifespan. However, tissue-level H and E from microindentation [30–34] and nanoindentation of cortical bone [34, 35] do not vary with donor age, though they do generally increase with tissue age [36, 37] or degree of mineralization (Table 1). As for *in vivo* microindentations of human tibia, the impact-derived BMSi was observed to increase with age (40 to 85 yo) when persons with and without fractures were included in the correlation [38]. However, in another study involving 46 Spanish and 42 Norwegian women with normal bone mineral density (20 to 79 yo), BMSi did not correlate with age [39]. More studies with large cohorts are necessary to determine if BMSi indeed decreases with advance aging.

Nano-mechanical properties of trabecular bone tissue also do not appear to vary much with age. Collecting 21 proximal femurs from male cadavers (17 to 82 yo), Ojanen et al. [40] conducted nanoindentation tests on *hydrated* trabecular bone from the femoral neck without

embedding the bone (ground and polished flat end of a core). For 10 unique trabeculae (5 tests per trabeculae), tissue was indented in force control to 30 mN, and in addition to H and E using the Oliver-Pharr (OP) method (Fig. 1) [41], they determined viscoelastic parameters during the dwell (60 s) using a Burgers rheological model of creep. Neither the elastic properties nor creep viscosity were associated with age [40]. Incidentally, in a similar nanoindentation study involving creep behavior of wet cortical bone (20 indents of interstitial and 20 indents of osteonal tissue per donor), Wu et al. [16] reported a significant difference in the exponential decay of creep between males (51 – 87 yo, n=10) and females (58 – 89, n=10) with no relationship to age. The functional significance of whether tissue quickly or slowly stops creeping is not immediately clear, though more viscosity would seemingly promote energy dissipation. In general, tissue-level properties rarely differ between females and males, especially not to the degree that structural properties differ between the genders, but the Wu et al. study does point out the importance of accounting for gender when assessing effects on tissue properties.

There are a few studies reporting differences in nanoindentation properties between age groups. Higher tissue hardness and modulus was observed for trabecular bone acquired from advanced aged, female donors (85 – 95 yo, n=5) in comparison to samples from aged, female donors (65 – 66 yo, n=5) [42]. The proximal femurs came from surgical cases involving femoral neck fractures and were extracted embedded in plastic, and so, all donors were likely osteoporotic, though the nature of the fracture (low-energy trauma) was not specified by the authors nor was the number of indents per donor per region. In a similar nanoindentation study of trabecular bone from femoral heads by another group, H and E of dry tissue, independent of depth, was higher for elderly female donors (83 – 94 yo, n=3) than for young female donors (27 – 38 yo, n=5)[43]. Unlike the other study, bones were collected during autopsy of donors without known skeletal diseases. Besides the small sample size, whether measurements from the indents (10 × 5 array per sample) were averaged or pooled in the statistical analysis was not specified.

From indentation tests of rodent bone, we know that tissue-level mechanical properties change with skeletal maturation if not with advanced aging. This was clearly demonstrated in a recent study in which embedded femur cross-sections from 70 male, Wistar rats throughout lifespan were indented by traditional nanoindentation (15 indents distributed throughout in the axial direction) [44]. Tissue-level H and E increased from 1-mo to 7-mo, but did not vary between 7-mo and 17-mo of age. As for aging in mice, Raghavan et al. [45] did not find a significant difference in H, E, or the plasticity index between 4-mo or 5-mo (n=21) and 19-mo (n=12) male, C57Bl/6 mice (combined non-exercised and exercised across age groups). The plasticity index, which varies over the range 0–1, is a measure of how much of the deformation is plastic, as opposed to elastic (and recoverable), and takes on larger values when the relative amount of plasticity is high. The indents were done on a smooth longitudinal surface created on the anterior side of wet femur mid-shafts (5 per bone in radial direction). The main finding from this study by Raghavan et al. was that the classification of young and aged mice required combining tissue-level properties, both mechanical and compositional, as their structure-function relationships varied in non-linear manner with age.

In an earlier study involving growing mice (1 day to 40 days of age), Miller et al. [46] indented rehydrated tibia cross-sections. Again, E was directly proportional to age (R^2=0.85) as primary mineralization principally occurs during adolescence. In higher order animals that experience significant osteonal remodeling, increases in H and E (female baboons) also occurred during sexual maturity [47], and storage modulus (E′) and loss modulus (E″) increased while the phase-shift (δ) decreased with maturation as observed from nanoindentation of dry humerus cross-sections acquired from growing New Zealand white rabbits between birth and 6-mo. [48]. Note that in all nanoindentation studies of bone, there are differences in the depth of indentation (specified force vs. specified depth), loading rate (force control vs. strain control), dwell period (10 s to 120 s), unloading rate (half of a fixed loading rate vs. loading rate approaching maximum depth), and dynamic parameters (hold force, force amplitude, and frequency). Still, average measurements of elastic and viscoelastic properties of bone tissue likely cannot, by themselves, explain the age-related increase in fracture risk.

Estrogen-related changes in tissue-level mechanical properties

Since fracture risk increases following menopause, estrogen withdrawal could deleteriously affect tissue properties along with the deterioration of trabecular microarchitecture. Investigating this possibility, Polly et al. [49] analyzed 15 paired transiliac biopsies prior to (49.0 ± 1.9 yo) and then 1-year (54.6 ± 2.2 yo) after cessation of menses. After grinding and polishing the fixed, embedded samples, quasi-static nanoindentation (dwell at 6 mN with an average depth of 770 nm) and dynamic nanoindentation (oscillating load during dwell with an amplitude between 75–125 μN and varying frequency in a step-wise manner) was performed at 25 unique sites within the trabeculae per specimen (analyzed the average for each donor). There were no statistically significant differences in H and E between pre-and post-menopause. For the most part, the dynamic properties did not significantly change following menopause, but the loss modulus (i.e., viscous dampening behavior) and tan δ (i.e., viscous energy dissipation) tended to be higher after menopause reaching significance for multiple, but not all, loading frequencies. Functionally, higher damping could be advantageous toward preventing fracture in the way it provides for greater energy dissipation through viscous deformation mechanisms [50].

Whether menopause has a permanent effect on tissue-level mechanical properties after turnover reaches an equilibrium remains to be determined, but generally, ovariectomy (OVX) to induce estrogen withdrawal in rats does not affect tissue-level H and E [51], though non-significant trends of lower H in OVX trabecular tissue can exist [52]. There is however one nanoindentation study comparing creep characteristics of hydrated tissue between sham-operated (n=6) and OVX rats (n=6) [53]. In this study, the effects of estrogen withdrawal occurred between 6-mo. and 8-mo. of age. Pooling nanoindentation values (not an average of tests within animal), the creep viscosity was higher for mandibular bone for OVX rats than for sham rats with no differences in viscosity or modulus between the groups when the lumbar vertebra was tested. Also, H and E of the cortical shell of lumbar vertebra was lower for OVX rats given a low protein diet compared to sham rats on a normal diet [54]. As for species in which osteonal remodeling is prominent, differences in cortical H and E (dry embedded femur cross-section) were observed between sham- and OVX-rabbits (7-

mo old at time of surgery with n=5 per time point) at 4 wks, 6 wks, and 8 wks post-surgery [55]. In an ovine OVX study, only E was reduced across trabeculae (cross-section) by estrogen withdrawal [56]. Also, feeding OVX rabbits (surgery at 16–17 wks) a methionine-rich diet for 16 weeks produced tissue in the mandible with lower storage modulus [57]. Fluorochrome labels were not administrated to quantify activation frequency in these OVX studies, but an increase in remodeling would explain why H, E, and the mineral-to-matrix ratio were all lower for the OVX than for the sham rabbits.

Osteoporosis-related differences in indentation-derived mechanical properties

Even though tissue-level H and E do not vary with age, they still may be affected by disease. Indentation properties of bone have been compared between osteoporotic individuals and otherwise healthy individuals (case-control matching for age and gender). In a study by Wang et al. [58], trabecular bone within iliac bone biopsies (dehydrated in ethanol, embedded in plastic, and tested dry) were acquired from Caucasian females who had sustained a vertebral fracture (68.4±5.1 yo, n=23) and who were considered healthy (64.4±5.4 yo, n=17). Taking the average of H and E within each specimen, these properties were not different between the two cases. However, when biopsies were reclassified based on dynamic histomorphometry, elastic modulus was higher for individuals with low (n=18) rather than high (n=22) bone formation rates per bone surface. In a follow-up study by the same group, significant differences in nano-mechanical properties were found between individuals taking bisphosphonates (BP) with severely suppressed bone turnover (SSBT) and age-matched controls but not between osteoporotic individuals (BP naïve) and age-matched controls [59]. The plastic deformation resistance, a parameter that accounts for effects of indenter geometry and elastic deformation on the measured hardness [56], of both trabecular and cortical bone was higher for SSBT than for controls. Other studies comparing tissue-properties of bone without a fracture (typically cadaver in origin) and bone near the site of fracture (e.g., femoral neck) did not find significant differences in nanoindentation properties [60, 61] (Table 2). One study reported lower E in the tissue of vertebral bodies from donors with very low BMD (n=6) than from donors with low-to-normal BMD (n=4) [62].

Seemingly, based on the cited studies, nano-mechanical properties do not contribute to fracture risk. However, when H and E are regressed against compositional properties as determined by qBEI or other imaging techniques probing tissue at the same-length scale as nanoindentation, relationships between E or H and mineralization differ between controls and fracture cases [60, 63] as in the case of aging mice [45]. For example, a lower E or H did not accompany a lower degree of mineralization (qBEI) within the femoral neck of fracture patients, relative to non-fracture controls, indicating changes to the organic matrix contributed to fragility [60]. Thus, even though E (tissue stiffness) or H (resistance to yielding) is not significantly different between osteoporotic and healthy bone, tissue-level mechanical properties may still contribute to fracture risk. For example, alterations in their relationship with composition (e.g., lower H for a given mineral-to-collagen ratio) could favor damage formation. Also, as discussed in a subsequent section, the heterogeneity in

both spatial and population distribution of modulus may favor or hinder toughening mechanisms.

While cRPI (BioDent) is currently not being advanced for clinical use, this technique was the first to assess tissue-level mechanical properties of human bone *in vivo*. The first reported case-control study involving cRPI (20 cycles at 11 N) [64] found that microindentation depth was significantly higher in female patients who recently sustained an osteoporosis-related fracture (79.1±7.5 yo, hip fracture n=25, vertebral fracture n=2) compared to control patients (83.2±5.3 yo, n=8) in the same hospital for non-fracture reasons. Using the same cRPI protocol, a second clinical study included 70 women divided into 4 groups: control patients (69±13 yo, n=20), long-term BP users (69±7 yo, n=6), patients with a typical hip osteoporotic fracture (BP naive, 82±9 yo, n=38), and patients with an atypical femoral fracture (long-term BP use, 74±6 yo, n=6) [65]. Consistent with the results of the first study, measurements of indentation distance into the periosteal bone were higher in fracture patients (whether typical or atypical) than in controls, after adjusting for age.

These minimally invasive, local indentation measurements assume that skeletal fragility is systemic, and therefore, a measurement at the tibia mid-shaft is representative of tissue properties at key fragility fracture sites. Jenkins et al.[66] undertook cRPI measurements (10 cycles up to 10 N) on femoral neck samples collected at surgery after low-trauma hip fracture (interquartile range 77–87 yo, n=46 with 17 males) and from cadaveric controls (interquartile range 61–74 yo, n=16 with 7 males). Again, bone from osteoporotic fracture patients was less resistant to microindentation than bone from controls, even after adjusting for cofounding factors (age, sex, BMI, and height). More importantly, this study confirms others' reports that cRPI measurements can detect skeletal fragility, independently of hip BMD [64, 67]. Milovanovic et al. [68] also indented femoral neck samples but did not observe significant differences in indentation depth between hip fracture patients and healthy controls, likely due to the small number of donors (5 fractures and 4 controls), the limited number of indents per bone (3 instead of ~8 to 15 for other studies) and the use of a particularly low target force (2 N).

Using IMI with the OsteoProbe instrument (the current technique being actively investigated for clinical use), Malgo et al. [38] conducted a case-control study involving a cohort of 90 patients ([40 – 86] yo) having either osteopenia (T-score <−1.0) or osteoporosis (T-score < −2.5). BMSi was lower in patients with a fragility fracture (n=63) compared with non-fracture subjects (n=27), independent of BMD. BMSi values also discriminated patients with different fracture status in the osteopenic group only. Discordantly, in another clinical study including 180 elderly women (78.3±1.1 yo, 117 with a history of fracture and 63 controls), BMSi was not associated with prevalent fractures [69]. However, several factors may explain the lack of sensitivity of the OsteoProbe to fracture status in this study: (i) fractures were self-reported, (ii) any fracture occurring after 50 years old was included so that several decades passed between the fracture event and the actual indentation testing, and (iii) 25% of reported fractures were not osteoporotic.

In addition to skeletal fragility, *in vivo* microindentation measurements may be sensitive to changes in bone tissue associated with pharmaceutical treatments or other diseases like diabetes. In a longitudinal study including 52 patients with glucocorticoid-induced osteoporosis, BMSi significantly increased for those treated with denosumab (n=15) and teraparatide (n=5) as early as 7 weeks and again at 20 weeks after the start of treatment [70]. Serving as a negative control, BMSi did not increase in patients receiving calcium and vitamin D supplementation only (n=19). BMSi was also reported to be lower for post-menopausal women with type 2 diabetes (n=30) than without diabetes (n=30). The difference was significant after adjusting for known risk factors of fracture [71]. To date, what BMSi is measuring or what attributes of bone tissue influence BMSi is not known.

Contribution of tissue-level mechanical properties to fracture resistance

Most tissue-level mechanical properties derived from quasi-static micro/nanoindentation tests do not typically correlate with mechanical properties of bone at the apparent level as determined by quasi-static, load-to-failure tests of uniform specimens [35]. In a recent study investigating these relationships across length scales, Mirzaali et al. [34] acquired fresh-frozen cadaveric femurs from 19 male and 20 female donors (46 to 99 yo) and machined mechanical specimens from the proximal end of the mid-shaft. Prior to machining, a cross-section and a transverse-section were cut, embedded and polished for nanoindentation. There were 10 indents per section with maximum depth of 1 μm. To determine whether nano-mechanical properties combined with microstructural features (bone volume fraction, cement line density, and mineral-to-matrix ratio) could explain the apparent-level mechanical properties, the data was fit to a power law relationship. Using backwards step-wise regression, only bone volume fraction significantly explained the variance in tensile strength and elastic modulus.

To clarify how cRPI properties relate to conventional testing methods, a number of *ex vivo* studies have compared cRPI outcomes to apparent-level material properties. Indentation depth assessed from cRPI on cadaveric femoral bone from 34 donors (65±25 [21–99] yo) was inversely correlated with both peak bending strength and toughness derived from three-point bend (3pt) testing [22]. Similar relationships were observed after conducting cRPI and 3pt testing on femurs from non-diabetic and diabetic rats sacrificed at 32 weeks of age (n=18) as well as on ribs from mature female beagles with and with BP-treatment (n=19) [72]. After adjusting for age, cRPI properties also helped the explain the 24–38% of the variance in fracture toughness properties (i.e. resistance to crack initiation and propagation) for a set of single-edge notched beams from 62 human femurs (64±22 [21–99] yo) [29]. On the other hand, Carriero et al. [73] argued that cRPI is not indicative of fracture toughness as indentation depths were higher in mouse bones with very brittle (*oim/oim*) and with very ductile (*Phospho1*$^{-/-}$) behavior, compared to their controls. However, since cRPI outcomes do not only reflect differences in fracture toughness, it is conceivable that the higher indentation depth observed in the *oim* model occurred because the brittle bone was susceptible to local damage generated by the probe, while the higher indentation depth observed in the *Phospho1*$^{-/-}$ model occurred because poorly mineralized bone with a reduced hardness lowered resistance to indentation.

The possible role of tissue heterogeneity in fracture resistance

Based on mechanisms well described in material physics [74], heterogeneity in a material (i.e. the spatial variation of structural and compositional properties in a material), can increase its resistance to fracture by various mechanisms including crack deflection/arrest and shielding from interfaces, which all require energy dissipation. On the other hand, extreme heterogeneity may concentrate strain in regions of low modulus, promoting crack initiation, and thereby hindering fracture resistance. In bone, tissue heterogeneity can change with age [75], bone remodeling rate [76] or drug therapy [77–79]. Therefore, loss of heterogeneity at the tissue-level has emerged as a possible factor contributing to an increased risk of fracture, a thesis supported by computational models that simulate crack propagation through cortical bone [80]. There is only one study to date however that investigated whether there are differences in nanoindentation heterogeneity between fracture and non-fracture cases, and only the standard deviation in cortical modulus and in cortical plastic deformation resistance was lower and higher, respectively for atypical fracture cases (long-term BP use giving rise to SSBT) than for age-matched non-fracture cases [59] (Table 2).

Since there is a practical limit to how many indents can be done to assess tissue heterogeneity, most studies have investigated whether differences in compositional heterogeneity exist between fracture patients and non-fracture controls. No consensus on whether heterogeneity increases or decreases fracture risk has emerged yet. In such studies (Table 2), heterogeneity is typically assessed as the full-width at the half maximum (FWHM) of the distribution of a compositional property (e.g. degree of mineralization, mineral-to-matrix ratio) because sampling is high enough to generate histograms with Gaussian-like distributions. As an example, microradiographs of bone sections extracted from the femoral neck of 23 women (82.7 yo [65–96]) who sustained a hip fracture and 14 cadaveric controls (86.9 yo [75–103]) showed a significantly higher heterogeneity in tissue mineralization in fracture patients compared with controls [81]. A similar observation was made by Tamminen et al. [82] in a pediatric population: heterogeneity in mineralization assessed from qBEI images of cross-sectional areas of transiliac bone biopsy from 24 children with idiopathic osteoporosis and a history of fractures (17 boys, 6.7 – 16.6 yo) was significantly higher compared to a normal reference data. On the contrary, in an infrared spectroscopy image (FTIR) analysis of femoral neck biopsies from 10 hip fracture cases (female 65 – 91 yo) and 10 age and sex-matched control necropsies (female 74 – 89 yo), heterogeneity of mineral-to-matrix and carbonate-to-phosphate ratios was significantly lower in the fracture than in the non-fracture group [83].

The association between heterogeneity in tissue composition and fracture risk in these imaging studies may not be causal as they do not adjust for major determinants of fracture risk, e.g. BMD or microarchitecture. Recently, in the largest FTIR imaging study to date involving iliac crest biopsies from age- and BMD-matched female subjects with (n=60) and without fracture (n=60) [84], heterogeneity of various outcomes (mineral-to-matrix ratio, carbonate-to-phosphate ratio, crystallinity, acid phosphate substitution, collagen maturity) was not significantly different between the two cases, whether analyzing the cortical or the cancellous tissue. Multivariate analyses on the matched data set suggested that an increase in collagen maturity heterogeneity was a significant independent predictor of fracture status,

although only in trabecular bone (p=0.0491). A common analysis technique – and possible limitation - to these studies is the use of the FWHM to assess tissue heterogeneity (i.e., a population heterogeneity that describes the variance of a metric over an entire region). Moving forward, including a measure of the region heterogeneity within a region (i.e., variograms), indicative of local contrast, may be more informative to explain the decreased resistance to fracture in a given individual.

Challenges and recommendations in the application of nanoindentation to bone

In dynamic nano-mechanical testing, the harmonic stiffness and phase angle depend not only on the viscoelastic characteristics of the bone tissue but also on the dynamic properties of the instrument. To accurately characterize the viscoelastic properties of bone specimens, it is thus necessary to correct the measured data for the influence of the instrument [85, 86]. Driving the indenter tip into the sample increases the stiffness and damping of the system. Therefore, the measured phase angle varies with indentation depth, even for a homogenous material. A dynamic nano-mechanical test that varies the oscillation frequency could observe a frequency-dependent material response, when in fact none exists. An important upshot of all of this is that the viscoelastic behavior of the instrument must be well characterized and carefully factored in in the data analysis procedures to obtain accurate measurements of viscoelastic properties. A simple way to characterize the machine dynamics is to oscillate the tip in air immediately prior to or after making an indent [85].

Another recommendation for the nanoindentation of bone is to not correct for thermal drift. The assumption behind the thermal drift calculation is that a change in displacement during the period in which load is held constant is due to thermal contraction or expansion of the material. However, viscoelastic materials such as bone exhibit time-dependent deformation. When an indenter is driven into bone tissue and then held at fixed load, it creeps deeper into the surface over time. Similarly, upon unloading to a fraction of the peak load, the indenter moves backward over time as the sample viscoelastically recovers, an effect that looks just like thermal drift but is not. The effect of the thermal drift correction on displacement response increases with an increase in the duration of the indent, so indents with slow loading rates or long hold periods are affected the most. Additionally, the thermal drift correction can substantially alter creep test results. Thermal effects on displacement response can be minimized in practice by adding a delay between the setting up and running of an experiment to allow the instrument and sample to reach a thermal equilibrium.

When not constrained by the length scale of a feature of interest, such as the width of a lamella, it is preferable to use larger indents over smaller ones. There are several reasons for this. As discussed previously, the relative contribution of the dynamic properties of the instrument is greater at smaller depths. This means that the effect of an error in the correction for the indenter’s influence on dynamic measurements decreases with larger indentation depths. Also, to best fit the assumptions of the damped harmonic oscillator model, it is desirable for the amplitude of the harmonic displacement to be a small fraction of the total depth. Another reason to prefer larger indents is that relative errors in the

calculated projected contact area due to effects like surface roughness, misidentification of the location of the surface during the approach of the indenter to the surface, or uncertainties in the tip area function (the precise geometry of the indenter tip) are reduced. Accurate measurements of the projected contact area are crucial to almost all nanoindentation property measurements [40].

Conclusion

Traditional tissue-level mechanical properties such as modulus and hardness do not appear to differ between healthy and fragile bone. There are several reasons for why these properties do not directly associate with fracture risk: heterogeneity due to remodeling, importance of microstructural features (e.g., porosity) to fracture resistance, and lack of sensitivity to various toughness mechanisms (e.g., crack deflection at an interface). However, as nanoindentation techniques are refined, our understanding of how tissue-level mechanical properties contribute to fracture risk is likely to improve. There are alternative techniques that have not been widely used to date, but could help establish how tissue-level mechanics contributes to overall fracture resistance. One technique involves compressing a micropillar of bone tissue. Ion beam milling is required to excavate the small column of bone tissue, which can then be compressed to failure using a nanoindenter with flat punch tip. Using this technique on bovine cortical bone, Schwidrzik et al. [87] observed plastic deformation of lamellae without visible damage. Another, perhaps less technically challenging technique is the nanoscratch in which a Berkovich tip is pressed into the bone tissue and pulled laterally across the bone surface. The work to scratch the bone was found to be less for older donors than for middle aged donors [88]. Also, removing proteoglycans from the surface of human cortical bone caused a reduction in this so-called in situ toughness [89]. Moving forward, advancing existing and emerging techniques is necessary to improve our understanding of how changes in tissue-level mechanical properties contribute to fracture risk.

References

Papers of particular interest, published recently, have been highlighted as:

*Of importance

**Of major importance

1. Lewis G, Nyman JS. The use of nanoindentation for characterizing the properties of mineralized hard tissues: state-of-the art review. Journal of biomedical materials research Part B, Applied biomaterials. 2008; 87(1):286–301.
2. Thurner PJ. Atomic force microscopy and indentation force measurement of bone. Wiley Interdiscip Rev Nanomed Nanobiotechnol. 2009; 1(6):624–49. [PubMed: 20049821]
3. Liu XS, Stein EM, Zhou B, Zhang CA, Nickolas TL, Cohen A, et al. Individual trabecula segmentation (ITS)-based morphological analyses and microfinite element analysis of HR-pQCT images discriminate postmenopausal fragility fractures independent of DXA measurements. J Bone Miner Res. 2012; 27(2):263–72. [PubMed: 22072446]
4. Nishiyama KK, Macdonald HM, Hanley DA, Boyd SK. Women with previous fragility fractures can be classified based on bone microarchitecture and finite element analysis measured with HR-pQCT. Osteoporos Int. 2013; 24(5):1733–40. [PubMed: 23179565]

5. Chang G, Honig S, Liu Y, Chen C, Chu KK, Rajapakse CS, et al. 7 Tesla MRI of bone microarchitecture discriminates between women without and with fragility fractures who do not differ by bone mineral density. Journal of bone and mineral metabolism. 2015; 33(3):285–93. [PubMed: 24752823]

6. Bergot C, Laval-Jeantet AM, Hutchinson K, Dautraix I, Caulin F, Genant HK. A comparison of spinal quantitative computed tomography with dual energy X-ray absorptiometry in European women with vertebral and nonvertebral fractures. Calcif Tissue Int. 2001; 68(2):74–82. [PubMed: 11310350]

7*. Orwoll ES, Marshall LM, Nielson CM, Cummings SR, Lapidus J, Cauley JA, et al. Finite element analysis of the proximal femur and hip fracture risk in older men. J Bone Miner Res. 2009; 24(3): 475–83. There is overlap in predicted hip strength between fragility fracture cases and non-fracture cases suggesting the tissue quality is also important to fracture risk. [PubMed: 19049327]

8. Chang G, Honig S, Brown R, Deniz CM, Egol KA, Babb JS, et al. Finite element analysis applied to 3-T MR imaging of proximal femur microarchitecture: lower bone strength in patients with fragility fractures compared with control subjects. Radiology. 2014; 272(2):464–74. [PubMed: 24689884]

9. Nishiyama KK, Ito M, Harada A, Boyd SK. Classification of women with and without hip fracture based on quantitative computed tomography and finite element analysis. Osteoporos Int. 2014; 25(2):619–26. [PubMed: 23948875]

10. Chevalley T, Bonjour JP, van Rietbergen B, Ferrari S, Rizzoli R. Fracture history of healthy premenopausal women is associated with a reduction of cortical microstructural components at the distal radius. Bone. 2013; 55(2):377–83. [PubMed: 23659831]

11. Imai K, Ohnishi I, Matsumoto T, Yamamoto S, Nakamura K. Assessment of vertebral fracture risk and therapeutic effects of alendronate in postmenopausal women using a quantitative computed tomography-based nonlinear finite element method. Osteoporos Int. 2009; 20(5):801–10. [PubMed: 18800178]

12. Graeff C, Marin F, Petto H, Kayser O, Reisinger A, Pena J, et al. High resolution quantitative computed tomography-based assessment of trabecular microstructure and strength estimates by finite-element analysis of the spine, but not DXA, reflects vertebral fracture status in men with glucocorticoid-induced osteoporosis. Bone. 2013; 52(2):568–77. [PubMed: 23149277]

13. Nyman JS, Makowski AJ. The contribution of the extracellular matrix to the fracture resistance of bone. Curr Osteoporos Rep. 2012; 10(2):169–77. [PubMed: 22527725]

14. Sroga GE, Vashishth D. Effects of bone matrix proteins on fracture and fragility in osteoporosis. Curr Osteoporos Rep. 2012; 10(2):141–50. [PubMed: 22535528]

15. Zysset PK. Indentation of bone tissue: a short review. Osteoporos Int. 2009; 20(6):1049–55. [PubMed: 19340511]

16. Wu Z, Ovaert TC, Niebur GL. Viscoelastic properties of human cortical bone tissue depend on gender and elastic modulus. J Orthop Res. 2012; 30(5):693–9. [PubMed: 22052806]

17. Maruyama N, Shibata Y, Wurihan, Swain MV, Kataoka Y, Takiguchi Y, et al. Strain-rate stiffening of cortical bone: observations and implications from nanoindentation experiments. Nanoscale. 2014; 6(24):14863–71. [PubMed: 25363088]

18. Hansma P, Turner P, Drake B, Yurtsev E, Proctor A, Mathews P, et al. The bone diagnostic instrument II: indentation distance increase. Rev Sci Instrum. 2008; 79(6):064303. [PubMed: 18601422]

19. Bridges D, Randall C, Hansma PK. A new device for performing reference point indentation without a reference probe. Rev Sci Instrum. 2012; 83(4):044301. [PubMed: 22559552]

20. Karim L, Van Vliet M, Bouxsein ML. Comparison of cyclic and impact-based reference point indentation measurements in human cadaveric tibia. Bone. 2015

21. Allen MR, McNerny E, Organ JM, Wallace JM. True Gold or Pyrite: A Review of Reference Point Indentation for Assessing Bone Mechanical Properties In Vivo. J Bone Miner Res. 2015

22. Granke M, Coulmier A, Uppuganti S, Gaddy JA, Does MD, Nyman JS. Insights into reference point indentation involving human cortical bone: Sensitivity to tissue anisotropy and mechanical behavior. J Mech Behav Biomed Mater. 2014; 37:174–85. [PubMed: 24929851]

23. Zebaze RM, Ghasem-Zadeh A, Bohte A, Iuliano-Burns S, Mirams M, Price RI, et al. Intracortical remodelling and porosity in the distal radius and post-mortem femurs of women: a cross-sectional study. Lancet. 2010; 375(9727):1729–36. [PubMed: 20472174]

24*. Abraham AC, Agarwalla A, Yadavalli A, Liu JY, Tang SY. Microstructural and compositional contributions towards the mechanical behavior of aging human bone measured by cyclic and impact reference point indentation. Bone. 2016 In press. Tissue-level mechanical properties from reference point microindentation of cadaveric tibia with soft tissue in place are weakly correlated with regional cortical porosoity.

25. Burstein AH, Reilly DT, Martens M. Aging of bone tissue: mechanical properties. J Bone Joint Surg Am. 1976; 58(1):82–6. [PubMed: 1249116]

26. McCalden RW, McGeough JA, Barker MB, Court-Brown CM. Age-related changes in the tensile properties of cortical bone. The relative importance of changes in porosity, mineralization, and microstructure. J Bone Joint Surg Am. 1993; 75(8):1193–205. [PubMed: 8354678]

27. Zioupos P, Currey JD. Changes in the stiffness, strength, and toughness of human cortical bone with age. Bone. 1998; 22(1):57–66. [PubMed: 9437514]

28. Nyman JS, Roy A, Tyler JH, Acuna RL, Gayle HJ, Wang X. Age-related factors affecting the postyield energy dissipation of human cortical bone. J Orthop Res. 2007; 25(5):646–55. [PubMed: 17266142]

29*. Granke M, Makowski AJ, Uppuganti S, Does MD, Nyman JS. Identifying novel clinical surrogates to assess human bone fracture toughness. J Bone Miner Res. 2015; 30(7):1290–300. Tissue-level mechanical properties from cyclic reference point microindentation help explain the variance ($R^2 \approx 30\%$) in fracture toughness when age is included as covariate. [PubMed: 25639628]

30. Houde J, Marchetti M, Duquette J, Hoffman A, Steinberg G, Crane GK, et al. Correlation of bone mineral density and femoral neck hardness in bovine and human samples. Calcif Tissue Int. 1995; 57(3):201–5. [PubMed: 8574937]

31. Hoffler CE, Moore KE, Kozloff K, Zysset PK, Goldstein SA. Age, gender, and bone lamellae elastic moduli. J Orthop Res. 2000; 18(3):432–7. [PubMed: 10937630]

32. Zioupos P, Gresle M, Winwood K. Fatigue strength of human cortical bone: age, physical, and material heterogeneity effects. J Biomed Mater Res A. 2008; 86(3):627–36. [PubMed: 18022837]

33. Wolfram U, Wilke HJ, Zysset PK. Rehydration of vertebral trabecular bone: influences on its anisotropy, its stiffness and the indentation work with a view to age, gender and vertebral level. Bone. 2010; 46(2):348–54. [PubMed: 19818423]

34**. Mirzaali MJ, Jakob Schwiedrzik J, Thaiwichai S, Best JP, Michler J, Zysset PK, et al. Mechanical properties of cortical bone and their relationships with age, gender, composition and microindentation properties in the elderly. Bone. 2015 in press. Tissue-level mechanical properties from quasi-static indentation tests do not help explain the variance in the apparent-level mechancial propeties of human cortical bone.

35. Rho JY, Zioupos P, Currey JD, Pharr GM. Microstructural elasticity and regional heterogeneity in human femoral bone of various ages examined by nano-indentation. J Biomech. 2002; 35:189–98. [PubMed: 11784537]

36. Donnelly E, Boskey AL, Baker SP, van der Meulen MC. Effects of tissue age on bone tissue material composition and nanomechanical properties in the rat cortex. J Biomed Mater Res A. 2010; 92(3):1048–56. [PubMed: 19301272]

37. Sinder BP, Lloyd WR, Salemi JD, Marini JC, Caird MS, Morris MD, et al. Effect of anti-sclerostin therapy and osteogenesis imperfecta on tissue-level properties in growing and adult mice while controlling for tissue age. Bone. 2016; 84:222–9. [PubMed: 26769006]

38**. Malgo F, Hamdy NAT, Papapoulos SE, Appelman-Dijkstra NM. Bone Material Strength as Measured by Microindentation In Vivo Is Decreased in Patients With Fragility Fractures Independently of Bone Mineral Density. The Journal of Clinical Endocrinology & Metabolism. 2015; 100(5):2039–45. Tissue resistance to impact microindentation of human subjects is lower for those with a fragility fracture than for those without a fracture. [PubMed: 25768670]

39. Duarte Sosa D, Vilaplana L, Guerri R, Nogues X, Wang-Fagerland M, Diez-Perez A, et al. Are the High Hip Fracture Rates Among Norwegian Women Explained by Impaired Bone Material Properties? J Bone Miner Res. 2015; 30(10):1784–9. [PubMed: 25900016]
40. Ojanen X, Isaksson H, Toyras J, Turunen MJ, Malo MK, Halvari A, et al. Relationships between tissue composition and viscoelastic properties in human trabecular bone. J Biomech. 2015; 48(2): 269–75. [PubMed: 25498367]
41. Oliver WC, Pharr GM. An improved technique for determining hardness and elastic modulus using load and displacement sensing indentation experiments. J Mater Res. 1992; 7(06):1564–83.
42. Gao J, Gong H, Zhang R, Zhu D. Age-related regional deterioration patterns and changes in nanoscale characterizations of trabeculae in the femoral head. Experimental gerontology. 2015; 62:63–72. [PubMed: 25582596]
43. Milovanovic P, Potocnik J, Djonic D, Nikolic S, Zivkovic V, Djuric M, et al. Age-related deterioration in trabecular bone mechanical properties at material level: nanoindentation study of the femoral neck in women by using AFM. Experimental gerontology. 2012; 47(2):154–9. [PubMed: 22155690]
44*. Zhang R, Gong H, Zhu D, Ma R, Fang J, Fan Y. Multi-level femoral morphology and mechanical properties of rats of different ages. Bone. 2015; 76:76–87. Tissue-level modulus and hardness increases with skeletal maturation but not with advanced aging in rodents. [PubMed: 25857690]
45*. Raghavan M, Sahar ND, Kohn DH, Morris MD. Age-specific profiles of tissue-level composition and mechanical properties in murine cortical bone. Bone. 2012; 50(4):942–53. The relationships between compositional and tissue-level mechanical properties change with advance agining in mice. [PubMed: 22285889]
46. Miller LM, Little W, Schirmer A, Sheik F, Busa B, Judex S. Accretion of bone quantity and quality in the developing mouse skeleton. J Bone Miner Res. 2007; 22(7):1037–45. [PubMed: 17402847]
47. Burket J, Gourion-Arsiquaud S, Havill LM, Baker SP, Boskey AL, van der Meulen MC. Microstructure and nanomechanical properties in osteons relate to tissue and animal age. J Biomech. 2011; 44(2):277–84. [PubMed: 21074774]
48. Isaksson H, Malkiewicz M, Nowak R, Helminen HJ, Jurvelin JS. Rabbit cortical bone tissue increases its elastic stiffness but becomes less viscoelastic with age. Bone. 2010; 47(6):1030–8. [PubMed: 20813215]
49. Polly BJ, Yuya PA, Akhter MP, Recker RR, Turner JA. Intrinsic material properties of trabecular bone by nanoindentation testing of biopsies taken from healthy women before and after menopause. Calcif Tissue Int. 2012; 90(4):286–93. [PubMed: 22349078]
50. Kim DG, Huja SS, Lee HR, Tee BC, Hueni S. Relationships of viscosity with contact hardness and modulus of bone matrix measured by nanoindentation. J Biomech Eng. 2010; 132(2):024502. [PubMed: 20370248]
51. Guo XE, Goldstein SA. Vertebral trabecular bone microscopic tissue elastic modulus and hardness do not change in ovariectomized rats. J Orthop Res. 2000; 18(2):333–6. [PubMed: 10815837]
52. Peng S, Liu XS, Huang S, Pan H, Zhen W, Zhou G, et al. Intervention timing of strontium treatment on estrogen depletion-induced osteoporosis in rats: bone microstructure and mechanics. J Orthop Res. 2014; 32(3):477–84. [PubMed: 24243710]
53. Kim DG, Huja SS, Navalgund A, D'Atri A, Tee B, Reeder S, et al. Effect of estrogen deficiency on regional variation of a viscoelastic tissue property of bone. J Biomech. 2013; 46(1):110–5. [PubMed: 23141522]
54. Hengsberger S, Ammann P, Legros B, Rizzoli R, Zysset P. Intrinsic bone tissue properties in adult rat vertebrae: modulation by dietary protein. Bone. 2005; 36(1):134–41. [PubMed: 15664011]
55. Wen XX, Wang FQ, Xu C, Wu ZX, Zhang Y, Feng YF, et al. Time Related Changes of Mineral and Collagen and Their Roles in Cortical Bone Mechanics of Ovariectomized Rabbits. PLoS One. 2015; 10(6):e0127973. [PubMed: 26046792]
56. Brennan O, Kennedy OD, Lee TC, Rackard SM, O'Brien FJ. Biomechanical properties across trabeculae from the proximal femur of normal and ovariectomised sheep. J Biomech. 2009; 42(4): 498–503. [PubMed: 19171344]

57. Ganeko K, Masaki C, Shibata Y, Mukaibo T, Kondo Y, Nakamoto T, et al. Bone Aging by Advanced Glycation End Products: A Multiscale Mechanical Analysis. Journal of dental research. 2015; 94(12):1684–90. [PubMed: 26310723]

58**. Wang X, Sudhaker Rao D, Ajdelsztajn L, Ciarelli TE, Lavernia EJ, Fyhrie DP. Human iliac crest cancellous bone elastic modulus and hardness differ with bone formation rate per bone surface but not by existence of prevalent vertebral fracture. J Biomed Mater Res Part B, Applied Biomater. 2008; 85(1):68–77. Tissue-level mechanical properties are not necessarily different between osteoporotic and otherwise normal bone. [PubMed: 17696151]

59*. Tjhia CK, Odvina CV, Rao DS, Stover SM, Wang X, Fyhrie DP. Mechanical property and tissue mineral density differences among severely suppressed bone turnover (SSBT) patients, osteoporotic patients, and normal subjects. Bone. 2011; 49(6):1279–89. The variance in tissue-level mechanical properties can be lower for patients with long-term bisphophonate use. [PubMed: 21958843]

60*. Fratzl-Zelman N, Roschger P, Gourrier A, Weber M, Misof BM, Loveridge N, et al. Combination of nanoindentation and quantitative backscattered electron imaging revealed altered bone material properties associated with femoral neck fragility. Calcif Tissue Int. 2009; 85(4):335–43. Tissue-level mechanical properties do not vary between osteoporotic and non-osteoporotic bone even though degree of mineralization was higher in the former than in the latter. [PubMed: 19756347]

61. Nazarian A, von Stechow D, Zurakowski D, Muller R, Snyder BD. Bone volume fraction explains the variation in strength and stiffness of cancellous bone affected by metastatic cancer and osteoporosis. Calcif Tissue Int. 2008; 83(6):368–79. [PubMed: 18946628]

62. Kim G, Cole JH, Boskey AL, Baker SP, van der Meulen MC. Reduced tissue-level stiffness and mineralization in osteoporotic cancellous bone. Calcif Tissue Int. 2014; 95(2):125–31. [PubMed: 24888692]

63. Tjhia CK, Stover SM, Rao DS, Odvina CV, Fyhrie DP. Relating micromechanical properties and mineral densities in severely suppressed bone turnover patients, osteoporotic patients, and normal subjects. Bone. 2012; 51(1):114–22. [PubMed: 22561877]

64. Diez-Perez A, Guerri R, Nogues X, Caceres E, Pena MJ, Mellibovsky L, et al. Microindentation for in vivo measurement of bone tissue mechanical properties in humans. J Bone Miner Res. 2010; 25(8):1877–85. [PubMed: 20200991]

65. Guerri-Fernandez RC, Nogues X, Quesada Gomez JM, Torres Del Pliego E, Puig L, Garcia-Giralt N, et al. Microindentation for in vivo measurement of bone tissue material properties in atypical femoral fracture patients and controls. J Bone Miner Res. 2013; 28(1):162–8. [PubMed: 22887720]

66. Jenkins T, Coutts LV, D'Angelo S, Dunlop DG, Oreffo RO, Cooper C, et al. Site-Dependent Reference Point Microindentation Complements Clinical Measures for Improved Fracture Risk Assessment at the Human Femoral Neck. J Bone Miner Res. 2015

67. Abraham AC, Agarwalla A, Yadavalli A, McAndrew C, Liu JY, Tang SY. Multiscale Predictors of Femoral Neck In Situ Strength in Aging Women: Contributions of BMD, Cortical Porosity, Reference Point Indentation, and Nonenzymatic Glycation. J Bone Miner Res. 2015; 30(12):2207–14. [PubMed: 26060094]

68. Milovanovic P, Rakocevic Z, Djonic D, Zivkovic V, Hahn M, Nikolic S, et al. Nano-structural, compositional and micro-architectural signs of cortical bone fragility at the superolateral femoral neck in elderly hip fracture patients vs. healthy aged controls. Experimental gerontology. 2014; 55:19–28. [PubMed: 24614625]

69. Rudang R, Zoulakis M, Sundh D, Brisby H, Diez-Perez A, Johansson L, et al. Bone material strength is associated with areal BMD but not with prevalent fractures in older women. Osteoporos Int. 2015

70. Mellibovsky L, Prieto-Alhambra D, Mellibovsky F, Guerri-Fernandez R, Nogues X, Randall C, et al. Bone Tissue Properties Measurement by Reference Point Indentation in Glucocorticoid-Induced Osteoporosis. J Bone Miner Res. 2015; 30(9):1651–6. [PubMed: 25736591]

71. Farr JN, Drake MT, Amin S, Melton LJ, McCready LK, Khosla S. In Vivo Assessment of Bone Quality in Postmenopausal Women With Type 2 Diabetes. J Bone Miner Res. 2014; 29(4):787–95. [PubMed: 24123088]

72. Gallant MA, Brown DM, Organ JM, Allen MR, Burr DB. Reference-point indentation correlates with bone toughness assessed using whole-bone traditional mechanical testing. Bone. 2013; 53(1): 301–5. [PubMed: 23274349]

73. Carriero A, Bruse JL, Oldknow KJ, Millan JL, Farquharson C, Shefelbine SJ. Reference point indentation is not indicative of whole mouse bone measures of stress intensity fracture toughness. Bone. 2014; 69C:174–9. [PubMed: 25280470]

74. Meisner MJ, Frantziskonis GN. Heterogeneous materials—Scaling phenomena relevant to fracture and to fracture toughness. Chaos, Solitons & Fractals. 1997; 8(2):151–70.

75. Yerramshetty JS, Lind C, Akkus O. The compositional and physicochemical homogeneity of male femoral cortex increases after the sixth decade. Bone. 2006; 39(6):1236–43. [PubMed: 16860007]

76. Boivin G, Farlay D, Bala Y, Doublier A, Meunier PJ, Delmas PD. Influence of remodeling on the mineralization of bone tissue. Osteoporos Int. 2009; 20(6):1023–6. [PubMed: 19340504]

77. Boskey AL. Bone composition: relationship to bone fragility and antiosteoporotic drug effects. Bonekey Rep. 2013; 2:447. [PubMed: 24501681]

78. Zoehrer R, Roschger P, Paschalis EP, Hofstaetter JG, Durchschlag E, Fratzl P, et al. Effects of 3- and 5-year treatment with risedronate on bone mineralization density distribution in triple biopsies of the iliac crest in postmenopausal women. J Bone Miner Res. 2006; 21(7):1106–12. [PubMed: 16813531]

79. Roschger P, Misof B, Paschalis E, Fratzl P, Klaushofer K. Changes in the degree of mineralization with osteoporosis and its treatment. Curr Osteoporos Rep. 2014; 12(3):338–50. [PubMed: 24947951]

80. Besdo S, Vashishth D. Extended Finite Element models of intracortical porosity and heterogeneity in cortical bone. Comp Mater Sci. 2012; 64:301–5.

81. Bousson V, Bergot C, Wu Y, Jolivet E, Zhou LQ, Laredo JD. Greater tissue mineralization heterogeneity in femoral neck cortex from hip-fractured females than controls. A microradiographic study. Bone. 2011; 48(6):1252–9. [PubMed: 21397739]

82. Tamminen IS, Misof BM, Roschger P, Mayranpaa MK, Turunen MJ, Isaksson H, et al. Increased heterogeneity of bone matrix mineralization in pediatric patients prone to fractures: a biopsy study. J Bone Miner Res. 2014; 29(5):1110–7. [PubMed: 24166885]

83. Gourion-Arsiquaud S, Lukashova L, Power J, Loveridge N, Reeve J, Boskey AL. Fourier transform infrared imaging of femoral neck bone: reduced heterogeneity of mineral-to-matrix and carbonate-to-phosphate and more variable crystallinity in treatment-naive fracture cases compared with fracture-free controls. J Bone Miner Res. 2013; 28(1):150–61. [PubMed: 22865771]

84**. Boskey AL, Donnelly E, Boskey E, Spevak L, Ma Y, Zhang W, et al. Examining the Relationships between Bone Tissue Composition, Compositional Heterogeneity and Fragility Fracture: A Matched Case Controlled FTIRI Study. J Bone Miner Res. 2015 in press. Heterogenetiy in composition does not differ between gender- and aBMD-matched fracture and non-fracture cases.

85. Herbert EG, Johanns KE, Singleton RS, Pharr GM. On the measurement of energy dissipation using nanoindentation and the continuous stiffness measurement technique. J Mater Res. 2013; 28(21):3029–42.

86. Herbert EG, Oliver WC, Pharr GM. Nanoindentation and the dynamic characterization of viscoelastic solids. Journal of Physics D: Applied Physics. 2008; 41(7):074021.

87. Schwiedrzik J, Raghavan R, Burki A, LeNader V, Wolfram U, Michler J, et al. In situ micropillar compression reveals superior strength and ductility but an absence of damage in lamellar bone. Nat Mater. 2014; 13(7):740–7. [PubMed: 24907926]

88. Islam A, Neil Dong X, Wang X. Mechanistic modeling of a nanoscratch test for determination of in situ toughness of bone. J Mech Behav Biomed Mater. 2012; 5(1):156–64. [PubMed: 22100090]

89*. Wang X, Xu H, Huang Y, Gu S, Jiang JX. Coupling Effect of Water and Proteoglycans on the In Situ Toughness of Bone. J Bone Miner Res. 2015 Removing proteoglycans lowers tissue-level toughness as determined by nano-scratch testing.

90. Pathak S, Vachhani SJ, Jepsen KJ, Goldman HM, Kalidindi SR. Assessment of lamellar level properties in mouse bone utilizing a novel spherical nanoindentation data analysis method. J Mech Behav Biomed Mater. 2012; 13:102–17. [PubMed: 22842281]

91. Loveridge N, Power J, Reeve J, Boyde A. Bone mineralization density and femoral neck fragility. Bone. 2004; 35(4):929–41. [PubMed: 15454100]
92. Sutton-Smith P, Beard H, Fazzalari N. Quantitative backscattered electron imaging of bone in proximal femur fragility and medical illness. J Microsc. 2008; 229(1):60–6. [PubMed: 18173645]
93. Carpentier VT, Wong J, Yeap Y, Gan C, Sutton-Smith P, Badiei A, et al. Increased proportion of hypermineralized osteocyte lacunae in osteoporotic and osteoarthritic human trabecular bone: implications for bone remodeling. Bone. 2012; 50(3):688–94. [PubMed: 22173055]
94. Ciarelli TE, Fyhrie DP, Parfitt AM. Effects of vertebral bone fragility and bone formation rate on the mineralization levels of cancellous bone from white females. Bone. 2003; 32(3):311–5. [PubMed: 12667559]
95. Ciarelli TE, Tjhia C, Rao DS, Qiu S, Parfitt AM, Fyhrie DP. Trabecular packet-level lamellar density patterns differ by fracture status and bone formation rate in white females. Bone. 2009; 45(5):903–8. [PubMed: 19615479]
96. Wu Y, Zhou L, Bergot C, Peyrin F, Bousson V. Cortical Bone Mineralization in the Human Femoral Neck in Cases and Controls from Synchrotron Radiation Study. Cell biochemistry and biophysics. 2015; 73(1):51–7. [PubMed: 25663507]
97. Gourion-Arsiquaud S, Faibish D, Myers E, Spevak L, Compston J, Hodsman A, et al. Use of FTIR spectroscopic imaging to identify parameters associated with fragility fracture. J Bone Miner Res. 2009; 24(9):1565–71. [PubMed: 19419303]
98. Wang ZX, Lloyd AA, Burket JC, Gourion-Arsiquaud S, Donnelly E. Altered distributions of bone tissue mineral and collagen properties in women with fragility fractures. Bone. 2016; 84:237–44. [PubMed: 26780445]

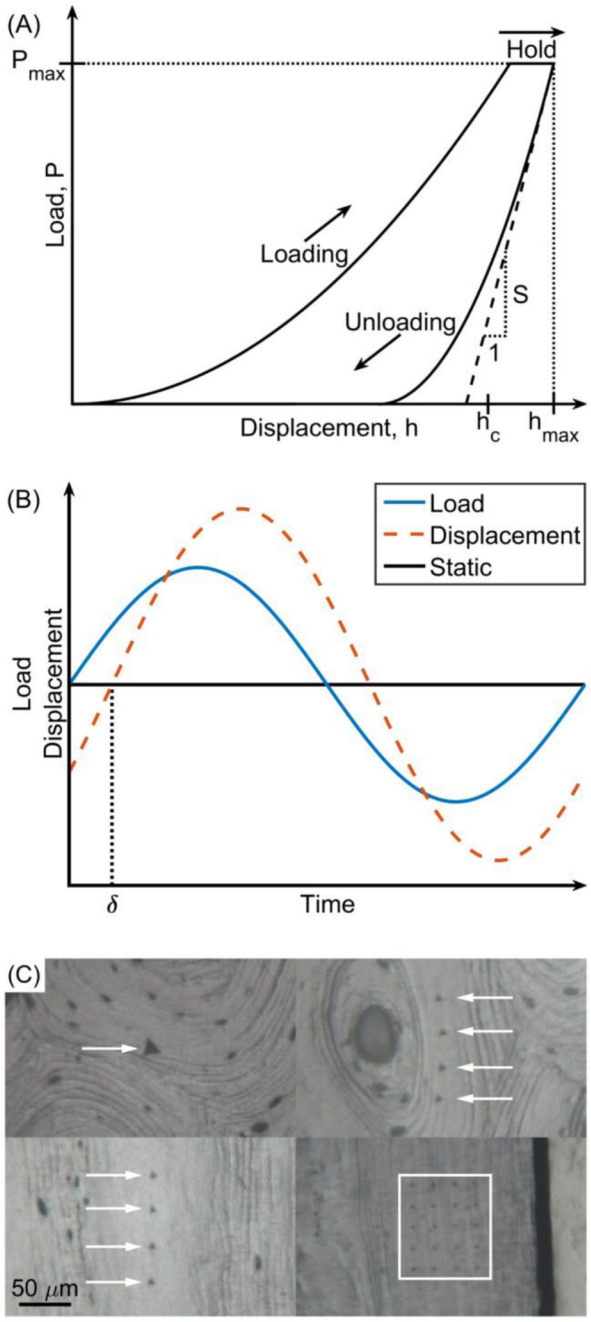

Figure 1.

Tissue-level mechanical properties are often determined from quas-static (a) or dynamic (b) nanonindentation tests of bone samples with polished surfaces (c). Arrows or a box mark the indents, which appear as triangles.

Curr Osteoporos Rep. Author manuscript; available in PMC 2017 August 01.

Table 1

Reported associations between indentation-derived properties and compositional properties acquired in the same region of bone.

Composition tool	Indentation (section; hydration)	Species (age)	Property	r-value	Property	Reference
FTIR	Nano-OP (transverse; wet)	mice (1–40 do)	MMR	0.77	E	[44]
			Cryst	0.48	E	
			CLR	−0.38	E	
Raman	Nano-OP (transverse, dry)	Rat (2 mo)	MMR	0.73	E	[34]
				0.79	H	
			CO_3/PO_4	0.60	E	
				0.63	H	
Raman	Nano-OP (transverse, dry?)	baboons (0.3–32.3 yo)	MMR	0.88	E	[45]
				0.84	H	
SHG			Col-Al	0.55	E	
Raman	Nano-OP (longitudinal; wet)	mice (4.5 mo)	CO_3/PO_4	0.77	PI	[43]
		mice (4.5 mo)	MMR	0.54	E	
		mice (19 mo)	MMR	−0.88 0.91	H PI	
		mice (4.5 mo)	CLR	−0.65 −0.60	E H	
Raman	Nano-S (transverse; dry)	mice (4 mo)	MMR	0.90	LE_s	[87]
				0.79	Y_{ind}	
				0.64	H	
Gravimetric	Nano-OP (transverse; wet)	human (51–89 yo)	ρ_{ash}	0.50	E_{int}	[16]
				−0.59	τ_{int}	
Inductively coupled plasma spectroscopy	Nano-OP (transverse; dry)	rat (1–17 mo)	Ca (%)	0.95	E	[42]
				0.98	H	
			P (%)	0.96	E	
				0.97	H	

Ca-peak is the degree of mineralization; FTIR is Fourier transform infrared microspectroscopy; E is modulus; H is hardness; Nano-OP is traditional nanoindentation using the Oliver-Pharr method to calculate H and E; CO_3/PO_4 is type B carbonate substitution; MMR is mineral-to-matrix ratio; PI is the plasticity index or slope of loading curve over the slope of the unloading curve; CLR is the cross-linking ratio (also known as matrix maturity ratio); Nano-S is nanoindentation using a diamond spherical tip and Hertzian contact model to convert P vs. h to stress vs. strain; LE_S is the elastic modulus as

determined from the loading slope in Nano-S; ρ_{ash} is bulk ash density; Y_{ind} is indentation yield strength; E_{int} is E of interstitial bone; τ_{int} is time constant of creep decay of interstitial bone; Col-Al is the relative degree of collagen alignment over lamellae; SHG is second harmonic generation microscopy.

Table 2

Associations between tissue composition or compositional heterogeneity and fracture risk

Technique	Type	Mean value fracture relative to control	Heterogeneity fracture relative to control	Resolution	Study population	Nature of fracture	Reference
BSE	Cort-FN Trab-FN	↓ Gray level	NR	5 μm	7 fracture (70–92y) 9 controls * (68–94y) All female	Intracapsular hip fracture	[88]
qBEI	Cort-FN	↓ Ca-Peak	NR	4 μm	5 fracture (74–92y) 5 controls * (75–88y) All female	Intracapsular hip fracture	[57]
qBEI	Trab-IT	↓ Ca	NR	1.7 μm	22 fragility fractures (12 female 73–101y; 10 male 59–94y) 22 controls (sex but not age-matched)	Subcapital femoral fracture	[89]
qBEI	Trab-IT	← Ca	NR	200×	14 osteoporotic fractures (10 F 74–91y; 4 M 65–94y) 15 controls (7 F 66–87y; 8 M 62–85y)	Subcapital femoral fracture	[90]
qBEI	Cort-sFN	↑ Ca-Peak	↓ Ca-Width	200×	5 fractures (82±4.6y) 5 controls * (82±9.8y) All female	Hip fracture (no antiresorp. treatment)	[65]
qBEI	Trab-IC	← Zmean	NR	300×	22 fractures (66.1±6.7y) 27 controls (63.7±5.3y) All female	Vertebral fracture	[91]
qBEI	Trab-IC	NR	↓ Ca-COV (low BFR)	0.76 μm	10 fracture high BFR 12 fracture low BFR 15 normal high BFR 12 normal low BFR	Vertebral fracture	[92]
Nanoindentation	Trab-IC Cort-IC	Fx + BP vs Control: No difference Fx − BP vs Control: No difference	Fx + BP vs Control: No difference Fx − BP vs Control: No difference	0.28 μm	12 fractures+BP (49–77 y.) 11 fractures, BP-free (53–76 y.) 12 controls * (49–74 y.) All female but one	Atypical fracture + BP Vertebral fracture, BP-free	[56]
qMR	Cort-iFN	↑ DMB	↑ variance DMB	2.63 μ	23 fracture (65–96y) 14 control (75–103y) All female	Intracapsular hip fracture	[78]
SR-μCT	Cort-iFN	← vDMB	← variance DMB	10.13 μm	23 fracture (65–96y) 17 control (72–103y) All female	Intracapsular hip fracture	[93]
FTIRI	Trab-IC Cort-IC	↑ XLR ↑ Carb (Cort-IC only) ← MMR ← XST	NR	6.25 μm	32 fractures (59±17y.) 22 controls (56±5y.) All female	Low-trauma fractures (no treatment for osteoporosis)	[94]
FTIRI	Cort-FN	↓ MMR ← Carb	↓ MMR ↑ XST	6.25 μm	10 fractures (65–91y.) 10 controls * (74–89y.)	Intracapsular hip fracture (BP naive)	[80]

Technique	Type	Mean value fracture relative to control	Heterogeneity fracture relative to control	Resolution	Study population	Nature of fracture	Reference
		← XLR ← XST			All female		
FTIRI	Trab-IC Cort-IC	↑ MMR (Trab-IC) ↑ XLR (Trab-IC)	XLR and XST: larger low-tail value (5th percentile)	6.25 μm	21 fractures (54±15y.) 4 controls (56±7y.) All female	Intracapsular hip fracture (BP and hormone replacement therapy naive)	[95]
FTIRI	Trab-IC Cort-IC	↑ Carb ← MMR ← XLR ← XST	No differences for any of the parameters	6.25 μm	60 fractures (62.2±7.4y.) 60 controls *† (61.8±7.3y.) All female	Fragility fractures (wrist, ankle, humerus, patella, shoulder, and other) BP or PTH treatment naïve	[81]
Nanoindentation	Cort-FN	← E, H	NR	4 μm	5 fracture (74–92y) 5 controls * (75–88y) All female	Intracapsular hip fracture	[57]
Nanoindentation	Trab-IC Cort-IC	Fx + BP vs Control: ↑ H, Hc in Trab-IC ↑ H in Cort-IC Fx − BP vs Control: No difference	NR	6 μm^2	12 fractures+BP (49–77 y.) 11 fractures, BP-free (53–76 y.) 12 controls * (49–74 y.) All female but one	Atypical fracture + BP Vertebral fracture, -BP	[56]

F: female; M: male; BSE: backscatter scanning electron microscopy; qBEI: quantitative backscatter electron imaging; qMR: quantitative microradiography; FTIRI: Fourier transform infrared spectroscopic imaging; IT: intertrochanteric; iFN: inferior femoral neck; sFN: superolateral femoral neck; IC: iliac crest biopsies; DMB: degree of mineralized bone; Ca-Peak: peak value of calcium distribution; Ca-Width: FWHM of calcium distribution; XLR: Collagen maturity ratio; XST: crystallinity; Carb: Carbonate substitution; MMR: Mineral-to-matrix ratio; FWHM: full width at half maximum; E: elastic modulus; H: plastic deformation resistance; Hc = contact hardness

*Age-matched cadaver;

†: BMD-matched cadavers